Modeling Light Propagation in a Smartphone's Under-Display Sensors

Qimeng Wang, Yi Liu*, Zihao Liang*, Haoteng Liu*, Bo-Ru Yang*, and Zong Qin**
***School of Electronics and Information Technology, Sun Yat-Sen University, Guangzhou, China**

Abstract
A universal light propagation model is built for a smartphone's under-display sensors. Under-display cameras, ambient light sensors, and proximity sensors are analyzed using the model. Far-field Fraunhofer diffraction, near-field geometric optics, and Fresnel diffraction are recognized, respectively. The model's effectiveness is experimentally verified for the three sensors.

Author Keywords
Under-display sensor; diffraction; optical simulation

1. Introduction
Bezel-less displays, *a.k.a.* infinity displays, enable smartphones with a high screen-to-body ratio for a better user experience. An essential obstacle to the infinity display is various sensors on the front side of a smartphone, such as the front camera, ambient light sensor (ALS), and proximity sensor. Placing the sensors under the display to achieve infinity displays elicits the concepts of under-display camera (UDC) and under-display sensing (UDS) [1-5]. Cameras and sensors work with light; however, as light must penetrate or be reflected by the screen, the complex structure of the display may cause diffraction, reflection, or absorption. For example, the UDC has not been widely commercialized mainly because of the diffraction-related image blurring caused by the semi-transparent display [5-8].

A light propagation model simulating how a UDC or UDS receives optical signals can help analyze received signals and optimize the sensor design. For example, our early studies [9,10] developed a full-color UDC simulator by adopting the Fraunhofer diffraction model. With its help, one can design new pixel structures with slighter diffraction [5,10-12] or quickly generate massive UDC images for training an image retrieval neural network [6,7,13]. Another example is the design of an under-display proximity sensor by Cai *et al*. [2]. They modeled the light emitted by an infrared source, reflected by the screen, and received by a detector. Based on the model, reflective diffraction was demonstrated to be the primary reason for noises when no human body approaches the smartphone. Furthermore, they optimized the sensor and detector's locations for lower noises. Sun *et al*. [4] calculated how rays are obstructed by black matrices (BM) to obtain the sensor's angular response for under-display ALS.

Despite the above efforts to model light propagation in UDC/UDS, a gap exists between current studies and rational design. First, some models only address typical conditions. For example, our previous UDC model based on Fraunhofer diffraction only accurately works for infinitely far objects and a camera lens closely attached to the display. An expansion to spherical incident waves and a lens away from the display is wanted [9,10]. More importantly, the light propagation behaviors in UDC and UDS are diverse. For instance, BM's geometric obstacles and diffraction were demonstrated to affect ALS and UDC, respectively [3,9]. In the face of diverse light sensors in a smartphone, few criteria have been set to indicate the applicable condition of the various models. Therefore, this study aims to build a universal framework for modeling light propagation in UDC/UDS. The front camera, ALS, and proximity sensor are analyzed by recognizing the fundamental underlying optical principle. The models are experimentally verified on a commercial smartphone.

2. Optical Principle
Fig. 1 shows the under-display camera, ALS, and proximity sensor configurations. Although they differ in whether the light source is inside or outside the display or whether light is reflected or penetrates, the common point is that a display panel lies on the path from the sensor's transmitter to its receiver. A priority in understanding light propagation is recognizing that the transmitter and receiver are in the display's far or near field. Accordingly, Fraunhofer diffraction and geometric optics should be adopted, respectively. For in-between cases, consider the Fresnel diffraction. The number of half-wave zones given in Eq. (1), *a.k.a.* the Fresnel number, can help determine the propagation mode.

$$N = \frac{a^2}{\lambda}\left(\frac{1}{z} + \frac{1}{z'}\right), \qquad (1)$$

where a is the aperture radius, z and z' are distances of the light source and observation plane from the aperture, and λ is the working wavelength. The aperture radius a should be counted in the region where a coherent light wave reaches.

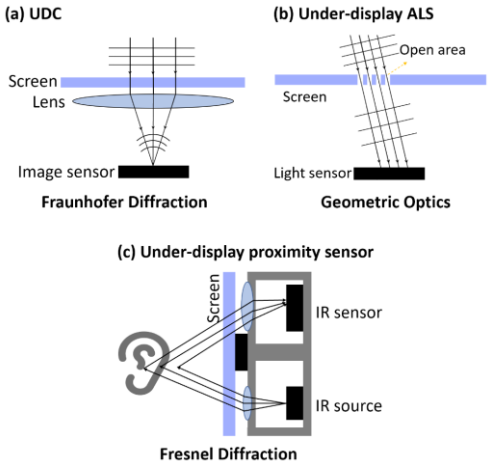

Fig. 1. Configurations of (a) UDC: Fraunhofer diffraction; (b) under-display ALS: geometric optics; (c) under-display proximity sensor: Fresnel diffraction.

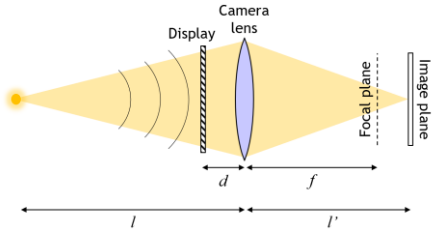

Fig. 2. Diffraction with a spherical incident wave and a camera lens away from the display.

ISSN 0097-996X/25/5602-1210-$1.00 © 2025

A Fresnel number much greater than one means that geometric optics dominates in the near-field, *a.k.a.* the shadow regime. At this point, raytracing-based simulation should be used, e.g., the ALS in Sec. 2.2, with its sensor very close to the display panel.

A Fresnel number smaller than one means far-field propagation, requiring Fraunhofer diffraction. Another thing to note is that Fraunhofer diffraction is established not only for a distant transmitter or receiver but also when a lens focuses light on its image plane, e.g., the image sensor covered by a lens in UDC.

For a Fresnel number moderately larger than one, the Fraunhofer diffraction evolves into Fresnel diffraction. Such propagation may occur in a proximity sensor whose IR transmitter emits a spherical wave. Although it is challenging to find analytical solutions for Fresnel diffraction, a practical approximate conclusion can be drawn for the modified Fraunhofer diffraction configuration shown in Fig. 2 [9]: the Fraunhofer diffraction pattern will be geometrically shrunk with a ratio equal to the distances of the light source to the display ($l - d$ in Fig. 2) and that to the camera lens (l). The configuration in Fig. 2 covers UDS working with Fresnel diffraction, so the conclusion will be adopted for the following analysis.

3. Verification

3.1 Under-display Camera (UDC)

UDC is a typical Fraunhofer diffraction case because a distant object emits a nearly-plane wave, and the camera is close to the display (d in Fig. 2 is zero). From a Fourier Optics point of view, the camera lens entirely separates angular wavevector components of incident light to redistribute them on the image sensor, so the frequency spectrum of the aperture function determines the point spread function (PSF). In particular, the periodic pixel structure attached to the camera aperture causes strong diffraction.

UDC simulators have been well-reported [9,12]. The general simulation method convolves the above diffracted PSF with an ideal image. Considering the wavevector is related to wavelength ($k = 2\pi \cdot \sin\theta/\lambda$), a full-color simulator sequentially calculates for different wavelengths and synthesizes into a chromatic image with the help of the luminous efficiency function and color matching function. Fig. 3 gives a simulation sample that highly resembles the experimental picture. The UDC image exhibits apparent diffraction fringes caused by the periodic pixel structure.

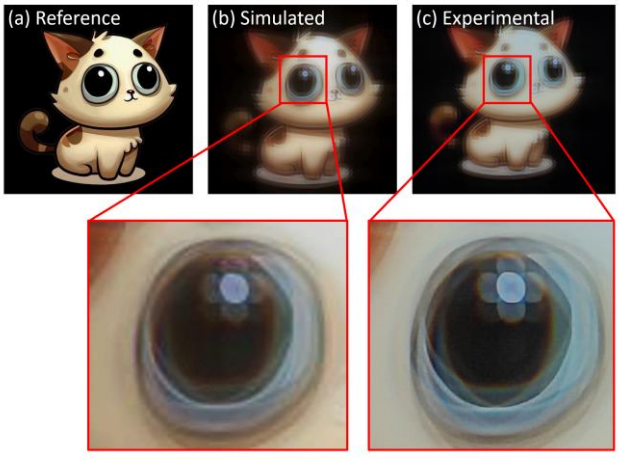

Fig. 3. (a) Reference, (b) simulated, and (c) experimental UDC images (aperture layout: rectangular; aperture ratio: 55%; pixel density: 254 ppi).

3.2 Under-display Ambient Light Sensor (ALS)

As Fig. 1(b) shows, an ALS contains a light sensor close to the screen to detect ambient brightness so that a smartphone can adjust the display brightness automatically. However, the angular response of under-display ALS considerably attenuates compared with regular ALS, which can be perfectly explained using the following geometric optics model.

Although ALS and UDC seem to have a similar configuration (compare Figs. 1(a) and (b)), the absence of a lens on the light sensor causes a fundamental difference. Using Eq. (1), the Fresnel number of such an ALS is larger than 2000 (z' is smaller than 1 mm), so geometric obstacles created by pixels are the root cause of the angular response attenuation. Pixels have absorptive side walls with a specific thickness d, as Fig. 4(a) shows. With increased incident angle θ, the side walls block more light. As a result, the response in large angles is reduced compared with regular ALS with a simple cosinoidal response curve.

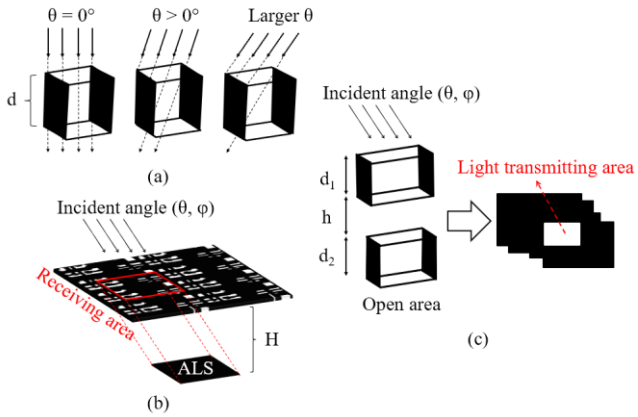

Fig. 4. (a) Geometric obstacles in under-display ALS. (b) Receiving area projected from the ALS. (c) Raytracing-based calculation of angular response for multiple layers

Corresponding to the above mechanism, the angular response is calculated using the following raytracing approach after acquiring the display's pixel layout using a transmissive microscope. (i) Along the direction (θ, φ) of incident light, project the sensor onto the lower surface of the display to obtain a display area where the sensor can receive the incident light, as the "receiving area" shown in Fig. 4(b). (ii) Project open areas in the pixel layout along (θ, φ) with the display thickness d to obtain the "light-transmitting areas" shown in Fig. 4(c). (iii) Add up all light-transmitting areas with weights of cosθ. (iv) For multiple layers, repeat (ii) and (iii) for every layer.

We adopt two commercial under-display ALS for experimental verification. The first is from a Vivo X70 smartphone with a 0.8-μm-thick pixel layer. The second one adopts color filters on encapsulation (COE), having a more complex multi-layer structure with a total thickness of 16.4 μm and a smaller aperture ratio. Figs. 5(a) and (b) show transmissive microphotographs of their pixel layouts, using which the corresponding angular responses are simulated and compared with experimental data, as Figs. 5(c) and (d) show. The experimental data is acquired using an LED lamp equipped on a stepping rotator. As a result, the simulation model exhibits very high accuracy, with an error smaller than 5 degrees in terms of full-width at half maximum (FWHM).

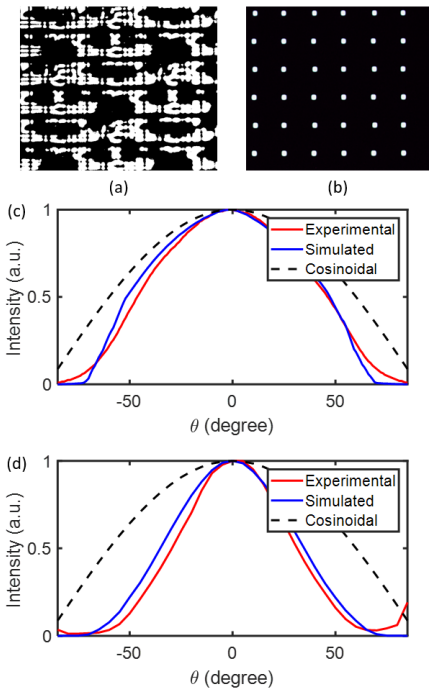

Fig. 5. Transmissive microphotographs of pixel layouts: (a) Vivo X70; (b) the COE display. (c) and (d) Simulated and experimental angular responses of the two ALS.

3.3 Under-display Proximity Sensor

The under-display proximity sensor detects a user's approach and turns off the touch sensor to avoid conflicting operations, enabled by an IR transmitter and an IR detector. Ideally, a proximity sensor only receives the light reflected by a foreign object, which then penetrates the screen. However, when nothing approaches the smartphone, the display sends back some IR light due to the under-display configuration, producing background noise.

Fig. 1(c) illustrates the proximity sensor to understand the root cause of background noise. Note that lenses are added on the transmitter and detector to collimate light for higher light utilization efficiency. The presence of lenses invalidates geometric optics, although the transmitter and detector are very close to the display. On the other hand, the transmitter is not placed on the image plane of the lens because no images are formed in this configuration, invalidating ideal Fraunhofer diffraction. Therefore, the reflective diffraction in the Fresnel regime produced by display pixels primarily affects the background noise.

According to the calculation method for Fresnel diffraction in Sec. 2, the diffraction pattern is shrunk from the ideal Fraunhofer pattern. Magnification is the distance of the light source to the display divided by that to the receiving lens. In the scenario of the under-display proximity sensor, Fig. 6(a) shows the geometry, where the light source is now the virtual image of the IR transmitter. Thus, the magnification equals to $D_1/(D_1+D_2)$.

We adopt the Vivo X70 and acquire its pixels' reflective microphotograph, as the diffraction is induced during reflection, as shown in Fig. 6(b). The reflective diffraction pattern is simulated with the magnification, as shown in Fig. 6(b). First, we analyze the role of the orientation between the IR transmitter (Tx) and the receiver (Rx) to validate the optical model. We simulate the background noise as a function of the Tx-Rx orientation, as shown in Fig. 6(d). As a result, the crosstalk is minimized under a 45-degree configuration, which can be explained by the directionality of the diffraction pattern of rectangularly arranged pixels. In contrast, simple reflection cannot explain the dependence on orientation. The conclusion agrees well with [2], suggesting that the 45-degree configuration is optimal concerning the pixel layout.

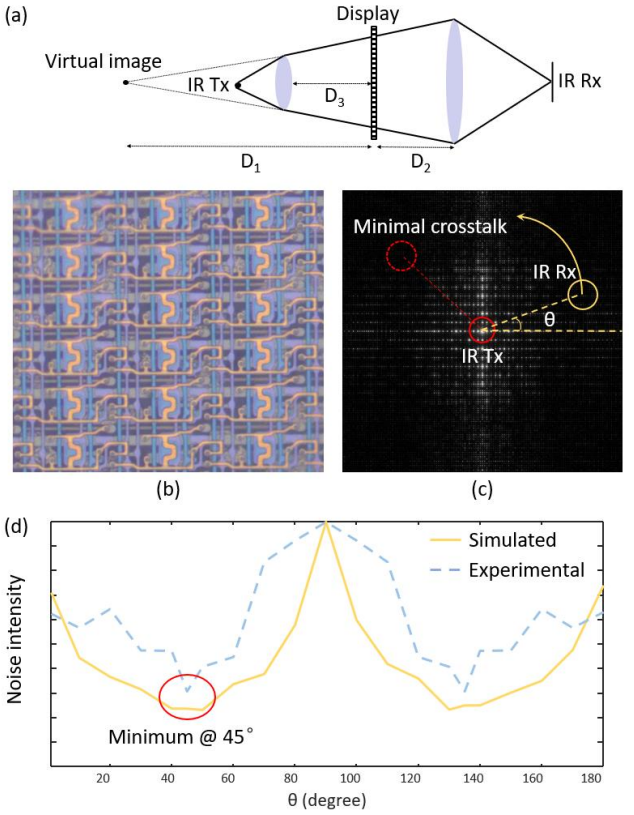

Fig. 6. (a) Geometry to calculate the diffraction pattern in the proximity sensor. (b) Reflective microphotographs of pixels. (c) Simulated reflective diffraction pattern. (d) Noise intensity as a function of the Tx-Rx orientation.

Another thing that significantly demonstrates that Fresnel diffraction dominates the background noise rather than geometric optics or Fraunhofer diffraction is the influence of the gap between the sensor and the display screen. If geometric optics dominate, the background noise will obey the inverse-square law with an increased gap, i.e., a rapid attenuation. However, we measure the noise as a function of the gap, i.e., D_3 in Fig. 6(a), and find that the noise smoothly increases with the gap. The Fraunhofer diffraction model cannot explain the increasing curve, either, because the Fraunhofer diffraction pattern is constant regardless of the sensor-display gap. On the other hand, we apply the Fresnel diffraction model with the magnification varying with the gap D_3. Here, the magnification equals $(D_1+D_3)/(D_1+D_2+2D_3)$. As a result, a similar increasing curve is obtained, proving the influence of Fresnel diffraction. The error between simulation and experiment may come from the difficulty in measuring D_3 in a smartphone.

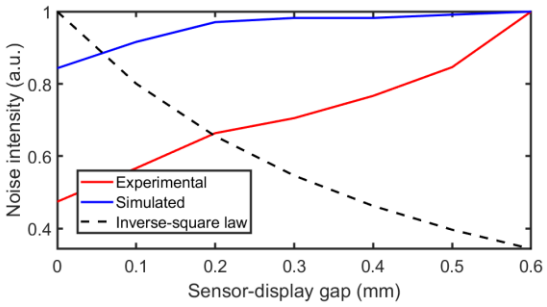

Fig. 7. Noise intensity as a function of the sensor-display gap. The dashed line shows the inverse-square law for reference.

4. Conclusions

Considering that various UDCs and UDSs in smartphones need a universal simulation model, this study provided a method to recognize the light propagation mode among geometric optics, ideal Fraunhofer diffraction, and Fresnel diffraction. An approximate but convenient calculation method for the Fresnel regime was also discussed. UDC, ALS, and proximity sensors were analyzed using the proposed model, which had highly matching results concerning experiments on commercial smartphones. In addition, other light-related problems in a smartphone also need rational analysis, such as the under-display ambient color sensor and ambient light reflection on the screen. The proposed light propagation model can be similarly applied.

References

[1] K. J. Vampola, G. Shao, W. Rieutort-Louis, M. Xu, M. Chappalli, and A. J. Roudbari, "12-1: Invited paper: Through-OLED display ambient color sensing," SID Symp. Dig. Tech. **53**(1), 117-120 (2022).

[2] W. Cai, C. Glazowski, L. Yan, et al., "54-1: Invited paper: Through OLED-display proximity sensing," SID Symp. Dig. Tech. **54**(1), 778-781 (2023).

[3] C.-C. Lai, W.-Y. Wang, Y.-C. Yuan, et al., "39-1: Designing high-sensitivity optical sensor for in-cell fingerprint sensor with thick cover glass in OLED display," SID Symp. Dig. Tech. **54**(1), 554-557 (2023).

[4] P.-L. Sun, Y.-Y. Chen, C.-T. Yueh, Y.-S. Li, Y.-C. Chang, C.-C. Lai, and C.-C. Lin, "P-82: Optimizing angular response and color estimation for LCD in-cell ambient light sensor," SID Symp. Dig. Tech. **54**(1), 1660-1663 (2023).

[5] A. Yang and A. C. Sankaranarayanan, "Designing display pixel layouts for under-panel cameras," IEEE T. Pattern Anal. **43**(7), 2245-2256 (2021).

[6] Y. Zhou, D. Ren, N. Emerton, S. Lim, and T. Large, "Image restoration for under-display camera," Proc. IEEE CVPR (2021), pp. 9179-9188.

[7] Y. Li, J. Wu, and Z. Shi, "Lightweight neural network for enhancing imaging performance of under-display camera." IEEE T. Circ. Syst. Vid. 34(1), 71-84 (2023).

[8] K. Gao, M. Chang, K. Jiang, Y. Wang, Z. Xu, H. Feng, Q. Li, Z. Hu, and Y. Chen, "Image restoration for real-world under-display imaging," Opt. Express **29**(23), 37820-37834 (2021).

[9] Z. Qin, Y.-H. Tsai, Y.-W. Yeh, Y.-P. Huang, and H.-P. D. Shieh, "See-through image blurring of transparent organic light-emitting diodes display: Calculation method based on diffraction and analysis of pixel structures," J. Disp. Technol. **12**(11), 1242-1249 (2016).

[10] Z. Qin, J. Xie, F.-C. Lin, Y.-P. Huang, and H.-P. D. Shieh, "Evaluation of a transparent display's pixel structure regarding subjective quality of diffracted see-through images." IEEE Photonics Journal **9**(4), 1-14 (2017).

[11] Z. Feng, Y. Wu, B. Surigalatu, X. Zhang, and K. Chang, "Large transparent display based on liquid crystal technology," Appl. Optics **59**(16), 4915-4920 (2020).

[12] Q. Yang, Z. Yang, Y.-F. Lan, and S.-T. Wu, "Low-diffraction transparent micro light-emitting diode displays with optimized pixel structure," J. Soc. Inf. Display **30**(5), 395-403 (2022).

[13] Z. Qin, R. Qiu, M. Li, X. Yu, and B.-R. Yang, "P-78: Simulator-based efficient panel design and image retrieval for under-display cameras," SID Symp. Dig. Tech. **52**(1), 1372-1375 (2021).